Journal of Applied Fluid Mechanics, Vol. 11, No. 6, pp. 1471-1476, 2018.
Available online at www.jafmonline.net, ISSN 1735-3572, EISSN 1735-3645.
DOI: 10.29252/jafm.11.06.28380

Sessile Drop on Oscillating Incline

L. De Maio and F. Dunlop†

Laboratory of Theoretical Physics and Modelling, CNRS UMR 8089 University of Cergy-Pontoise, 95302 Cergy-Pontoise, France

†*Corresponding Author Email: francois.dunlop@u-cergy.fr*

(Received September 7, 2017; accepted May 6, 2018)

ABSTRACT

Natural or industrial flows of a fluid often involve droplets or bubbles of another fluid, pinned by physical or chemical impurities or by the roughness of the bounding walls. Here we study numerically one drop pinned on a circular hydrophilic patch, on an oscillating incline whose angle is proportional to sin(ω*t*). The resulting deformation of the drop is measured by the displacement of its center of mass, which behaves similarly to a driven over-damped linear oscillator with amplitude *A*(ω) and phase lag φ(ω). The phase lag is *O*(ω) at small ω like a linear oscillator, but the amplitude is $O(\omega^{-1})$ in a wide range of large ω instead of O(ω−2) for a linear oscillator. A heuristic explanation is given for this behaviour. The simulations were performed with the software Comsol in mode Laminar Two-Phase Flow, Level Set, with fluid 1 as engine oil and fluid 2 as water.

Keywords: Droplet; Pinning; Two-Phase flow; Driven oscillator; Finite elements; Computational study.

1. INTRODUCTION

Equilibrium of a drop pinned on an incline was studied by many authors, see (De Coninck, Dunlop, and Huillet 2017) and references therein. Shape and motion of drops sliding down an inclined plane have also been studied, see (Le Grand, Daerr, and Limat 2005) and references therein. Drops on vibrating horizontal surfaces have been the subject of much interest recently from experimental, theoretical or numerical points of view. The vibrations or oscillations of the substrate can be horizontal (Daniel, Chaudhury, and de Gennes 2005; Lyubimov, Lyubimova, and Shklyaev 2004; Dong, L., Chaudhury, A., and Chaudhury, M. K. 2006; Celestini and Kofman 2006), or vertical (Lyubimov, Lyubimova, and Shklyaev 2006). The effect of vibrations on hysteresis, pinning and depinning, was studied in particular by (Noblin, X., Buguin, A., and Brochard-Wyart, F. 2004; Vukasinovic, Smith, and Glezer 2007). The effect of vibrations on the Cassie-Wenzel transition was studied in particular by (Boreyko and Chen 2009; Bormashenko, Pogreb, Whyman, and Erlich 2007). A review of drop oscillations is given by (Milne, Defez, Cabrerizo-Vlchez, and Amirfazli 2014). More recent experimental results and references are found in (Rahimzadeh and Eslamian 2017).

Here we consider the case of an oscillating incline where the angle α(*t*) of the slope follows

$$\alpha(t) = \frac{\pi}{4}\sin(\omega t) \tag{1}$$

while the circular basis of the drop remains fixed on the incline as a disc of radius *r*. We keep the frame of reference attached to the incline, so that the gravity vector oscillates:

$$g = \begin{pmatrix} g\sin(\alpha(t)) \\ 0 \\ -g\sin(\alpha(t)) \end{pmatrix} \tag{2}$$

We assume that the inertial pseudo-forces per unit volume, like the centrifugal force, are negligible with respect to gravity, which will be the case if $\omega^2 r \ll g$.

The Bond number is the ratio between gravity and capillarity, and we define it precisely as

$$Bo = \frac{\Delta\rho g r^2}{\sigma} \tag{3}$$

where Δρ is the density difference between the two fluids and σ is the interface tension. We are interested in moderate but significant drop deformations, with Bond number of order one, as shown on Fig. 1. All the simulations presented here

will be with Bo = 0.22. For bond number of order one and pulsation ω not much larger than the natural pulsation of the drop, the fluid velocity will vary from 0 to about ωr over a distance r. This motivates a Reynolds number defined as

$$Re_{\omega}=\frac{\rho\omega r^2}{\eta} \tag{4}$$

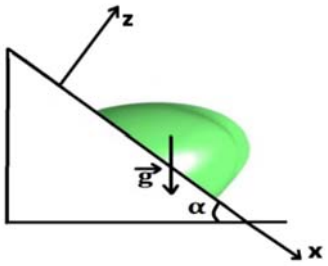

Fig. 1. Water drop at equilibrium pinned on incline of angle α = π/4. Bond number *Bo*=0.22. The drop is surrounded by oil.

with $\rho = \rho_{water}$ and $\eta = \eta_{water}$. In the same regime the quadratic term in the Navier-Stokes equation (5) will be of order $\rho\omega^2 r$, the same as the centrifugal force per unit volume. Therefore it will be consistent, and will save some computing time, to neglect it (Stokes flow). The equation remains non-linear due to the interfacial tension force.

For pulsations ω larger than the natural pulsation of the drop, the response of the drop and the actual velocity will be much smaller. A Reynolds number using the maximum measured velocity will always be less than 1 in our simulations. Viscosity plays an essential role in the present study, which does not allow short-cuts such as interface motion by curvature based on the Laplace-Young equation.

2. DIFFUSE INTERFACE AND LEVEL SET METHOD

The sharp interface between immiscible fluids is replaced by a diffuse interface spreading over a few mesh elements across the physical interface. A level set function φ, φ inspired by van der Waals, goes smoothly from zero to one when crossing the interface from fluid 1 into fluid 2. The mixture obeys the Navier-Stokes equation for an incompressible fluid,

$$\rho\frac{\partial u}{\partial t}+\rho(\mathrm{u}\cdot\nabla)\mathrm{u}=\nabla\cdot\left[-p\mathrm{I}+\eta\left(\nabla\mathrm{u}+\nabla\mathrm{u}^T\right)\right]+\rho\mathrm{g}+\mathrm{f}_{st} \tag{5}$$

$$\nabla\cdot\mathrm{u}=0 \tag{6}$$

where **I** is the identity matrix, and we neglect the quadratic term in (5). The density and dynamic viscosity are functions defined by

$$\begin{aligned}\rho&=(1-\phi)\rho_1+\phi\rho_2\\ \eta&=(1-\phi)\eta_1+\phi\eta_2\end{aligned} \tag{7}$$

The surface tension force per unit volume f_{st} is

$$\mathrm{f}_{st}=\nabla\cdot\left(\sigma\left(\mathrm{I}-\left(\mathrm{N}_{\phi}\mathrm{N}_{\phi}^T\right)\right)\delta\right) \tag{8}$$

where **σ** is the interfacial tension, $N\phi = \nabla\phi/|\nabla\phi|$is a normal vector also defined in the bulk, and $\delta = 6|\nabla\phi|\phi(1-\phi)$ is a smooth Dirac delta function concentrated near the interface, which is the level set $\{\phi = 0.5\}$. Formula (8), being the divergence of a flux, can be integrated by parts in the weak form of the partial differential equation, and then requires just one derivative of φ. It was shown by (Lafaurie, Nardone, Scardovelli, Zaleski, and Zanetti 1994) to be a smooth approximation to the usual Laplace force σHNφδ(interface) where H is the mean curvature of the interface and δ(interface) is a true Dirac delta function supported by the interface.

The level set function φ obeys

$$\frac{\partial\phi}{\partial t}+\mathrm{u}\cdot\nabla\phi=\gamma\nabla\cdot\left(\varepsilon\nabla\phi-\phi(1-\phi)\frac{\nabla\phi}{|\nabla\phi|}\right) \tag{9}$$

where ε in the diffusion term controls the interface thickness. It will be taken as h/2, half the mesh size. The parameter γ is a constant with the dimension of a velocity, which we fix as $r\omega/(2\pi)$ where r is the initial radius of the drop. The level set method for two phase flow was developed in particular by (Olsson and Kreiss 2005).

3. SETUP

The incline is designed with a circular hydrophilic patch of radius r = 2.5mm and the remaining surface hydrophobic. The corresponding Young contact angles are set to 0 degree (perfectly hydrophilic) and 180 degrees (perfectly hydrophobic) respectively.

A water drop of volume $2\pi r^3/3$ is deposited on the hydrophilic patch. The vessel is filled with oil, and closed with no air inside. In the absence of gravity, the drop is a hemisphere, with contact angle π/2. This will also be the initial configuration in our simulations.

The vessel is intended to be large with respect to the water drop, so that friction occurs only near the drop. The Archimedes force, encapsulated in the pressure and gravity terms of the Navier-Stokes equation, does not depend upon the volume of the vessel. For simulation purposes, we have to use a simulation box of modest size. The effect of the box will be minimized if it has the symmetry of the problem at lowest order, hence a hemisphere with same center as the initial drop, and we choose its radius as four times the initial drop radius. On it we choose "slip" boundary conditions: impenetrable and frictionless, again to minimize the effect of having a relatively small simulation box.

The center of the hydrophilic patch is chosen as origin of coordinates and the z-axis perpendicular to the incline. The incline then starts oscillating around the y-axis according to (1). The plane $\{y = 0\}$ is a plane of symmetry, allowing to make the study in a quarter of a sphere, see Fig. 2.

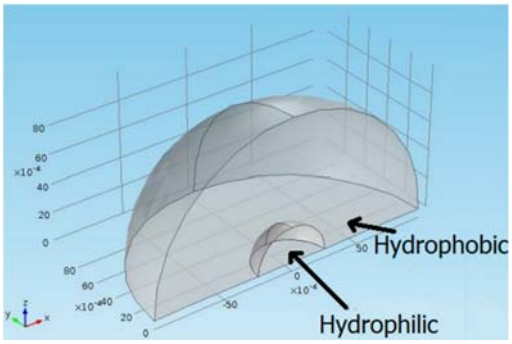

Fig. 2. Setup.

In the stationary regime, the contact angles at the front ($x = r$) and at the back ($x = -r$) will oscillate between a minimum angle θ^{min} and a maximum angle θ^{max}. So long as the maximum contact angle remains strictly less than 180 degrees, the contact line cannot move into the hydrophobic region. So long as the minimum contact angle remains strictly larger than 0 degree, the contact line cannot move into the hydrophilic region. The role of the substrate is to ensure pinning.

For real substrates, the advancing angle θ^A of the hydrophobic material and the receding angle θ^R of the hydrophilic material will replace 180 degrees and zero degree respectively. The scope of our study is bounded by the conditions

$$0 \le \theta^R < \theta^{min} < \theta^{max} < \theta^A \le \pi. \tag{10}$$

It implies bounds on Bond number and slope angle α, which are satisfied in the present study. It would be interesting to go beyond and also study depinning. This is left to future work.

Table 1 Physical parameters

	$\rho\left[\mathrm{kg/m^3}\right]$	$\eta\left[\mathrm{Pa\,s}\right]$	$\sigma\left[\mathrm{N/m}\right]$
Engine oil	888	0.079	
Water	1000	0.001	
Interface			0.031

4. COMSOL

We used the finite elements software Comsol (see https://www.comsol.com/) in mode Laminar Two-Phase Flow, Level Set, with fluid 1 as engine oil and fluid 2 as water, at 20°C, see Table 1. The simulation box is a quarter of a sphere of radius $4r$. The outer sphere is not a physical boundary, and on it we choose *slip* boundary conditions:

$$\mathrm{u}\cdot\mathrm{n} = 0$$

$$\mathrm{K} = \left(\mathrm{K}\cdot\mathrm{n}\right)\cdot\mathrm{n}, \qquad \mathrm{K} = \eta\left(\nabla\mathrm{u} + \nabla\mathrm{u}^T\right)\mathrm{n} \tag{11}$$

where K is the viscous stress vector upon an infinitesimal surface of normal **n**. The symmetry plane $\{y = 0\}$ obeys the same boundary conditions, with also

$$\nabla\cdot\mathrm{N}_\phi = 0 \tag{12}$$

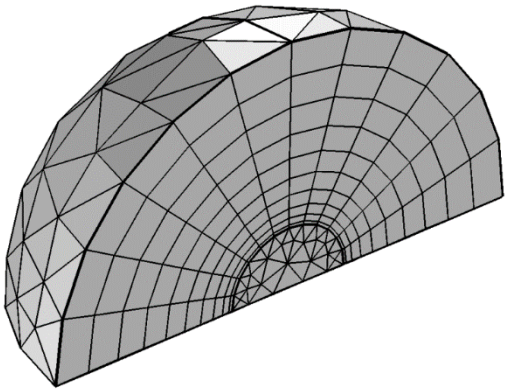

Fig. 3. Mesh.

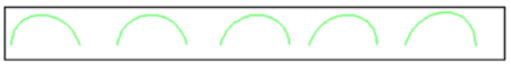

Fig. 4. Trace of the drop on the symmetry plane $\{y = 0\}$ at five times. *Bo*=0.22, ω=0.1s^{-1}.

The hydrophilic patch is a wetted wall with contact angle $\theta_w = 0$, meaning a boundary condition

$$\sigma\left(\mathrm{n} - \mathrm{N}_\phi\cos\theta_W\right)\delta = \frac{\eta}{\beta}\mathrm{u} \tag{13}$$

where β is a slip length equal to the mesh size h. The remaining part of the incline is a wetted wall with contact angle $\theta_w = \pi$. The mesh is built as shown on Fig. 3, with maximal mesh size h = 0.4 mm and $h \sim 0.1$ mm in the region of the interface, leading to 24560 degrees of freedom.

We impose at least one time step in every 1/40 of a period so as to be able to distinguish a sinusoidal response. With the chosen mesh, it turns out that Comsol does not need smaller time steps to satisfy its default tolerance. Each run for one value of ω took about 20 hours with an Intel i7-3770 CPU@3.40GHz x8.

5. RESULTS

The trace of the drop on the symmetry plane $\{y=0\}$ at different times is shown on Fig. 4. A film is also available on arXiv.

The contact angles $\theta^r(t)$ and $\theta^{-r}(t)$ at the front and the back are shown on Fig. 5. These contact angles are measured as

$$\theta = \arccos\left(\mathrm{n}\cdot\mathrm{N}_\phi\right) \tag{14}$$

at $(x,y,z) = (r,0,0)$ and $(x,y,z) = (-r,0,0)$ respectively. When the incline is set in motion, at $t = 0$, the liquid drop does not follow instantaneously, whence a start below 90 degrees. In the stationary regime a noticeable feature is that the contact line spends more time near the minimum than near the maximum.

Equation (14) is a measurement of the interface normal, pointing from oil into water, at a single

point, which is a mesh vertex. Small numerical errors are clearly visible in Fig. 5. A systematic error is also present: when the contact angle approaches θ^{max}, the contact line goes slightly into the hydrophobic region. Similarly when the contact angle approaches θ^{min}, the contact line goes slightly into the hydrophilic region. Measuring the contact angles at $x = \pm r$ underestimates the amplitude of oscillations.

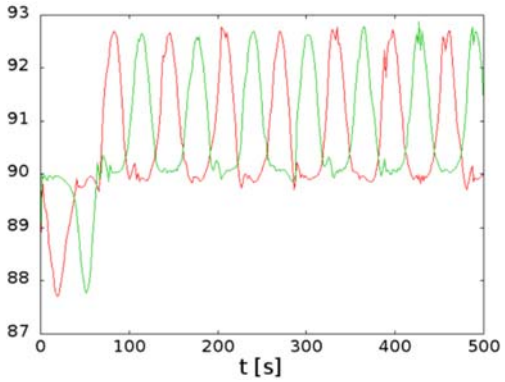

Fig. 5. Contact angles $\theta^{r}(t)$ at the front (red) and $\theta^{-r}(t)$ at the back (green), measured in degrees as (14), for *Bo* = 0.22, ω = 0.1s^{-1}.

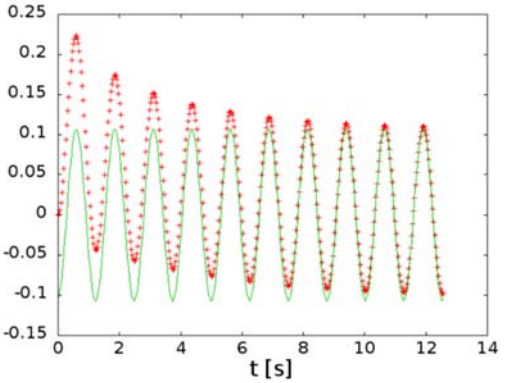

Fig. 6. Normalized abscissa of water center of mass $\bar{x}(t)$, as Eq. (15) (red +), and sinusoidal fit of permanent regime, A sin(ω*t* −φ) as (16) (green, continuous), for *Bo* = 0.22, ω = 5s^{-1}.

Measuring contact angles, experimentally or numerically, is subject to debate, especially in dynamics. Fitting individual images of a film is tedious and systematic deviations may also be present if the fit is over a length where gravity produces bending. In dynamics the bending effect of gravity cannot be computed exactly. We have therefore chosen to analyse the data in terms of the motion of the centre of mass of the drop, whose definition is obvious and whose statistics is optimal.

The abscissa of the center of mass of water is recorded, normalized arbitrarily using the drop basis radius r and the volume $\pi r^3/3$ of a quarter of a sphere of radius r:

$$\bar{x}(t) = \frac{\int dxdydz\,\phi(x,y,z,t)\,x}{\pi r^4/3} \qquad (15)$$

The integral is over the simulation box, namely a quarter of a sphere of radius 4r. After a transient, which lasts longer for larger ω, the system approaches a stable permanent regime, as shown on Figs. 6, 7. The finite elements method does not conserve exactly the total mass of each fluid, and a small parasitic drift is often present in simulations, but it is not the case here.

We then use the *gnuplot* fit, a nonlinear least-squares Marquardt-Levenberg algorithm, and search for an amplitude A and a phase lag φ such that

$$\bar{x}(t) - A\sin(\omega t - \varphi) \to 0 \quad \text{as} \quad t \to \infty \qquad (16)$$

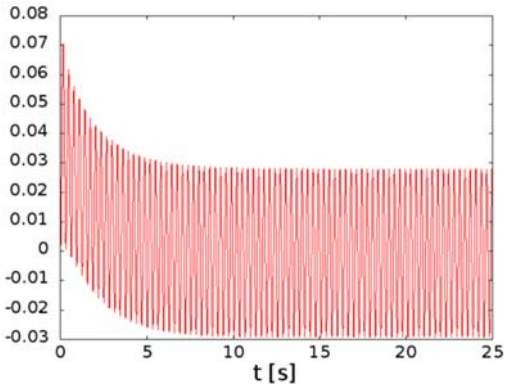

Fig. 7. Normalized abscissa of water center of mass $\bar{x}(t)$, Eq. (15), for ω = 20s^{-1}.

Table 2 results

$\omega\left[s^{-1}\right]$	A	$\varphi[\mathrm{rad}]$
0	1.92	0
0.05	1.89	0.275
0.1	1.68	0.503
0.2	1.25	0.79
0.5	0.66	1.06
1	0.387	1.17
2	0.228	1.24
5	0.105	1.41
10	0.0564	1.55
20	0.0286	1.66

Results are like the example shown on Fig. 6, where the error measured by the *rms* of residuals over one period falls below 1% after a few periods (after 7 periods in the example shown). The resulting incertainties over A and φ are also below 1%.

A sinusoidal response with the same ω as the incline angle was to be expected for a linear system. We used the Stokes equation with a non-linear surface tension force, and the transport equation (5) is also non-linear.

Results are listed in Table 2, where the case ω = 0 is in fact the limit as ω → 0, namely the stationary case $\alpha(t) = \pi/4\ \forall t > 0$. Plots of A and φ versus ω are given in Figs. 8 and 9. They look much like a driven

over-damped linear oscillator, with a notable exception: the amplitude of the permanent oscillations behaves like ω^{-1} at large ω instead of ω^{-2} for the driven damped linear oscillator. The phase lag $\varphi(\omega)$ is proportional to ω at small ω like a driven damped linear oscillator.

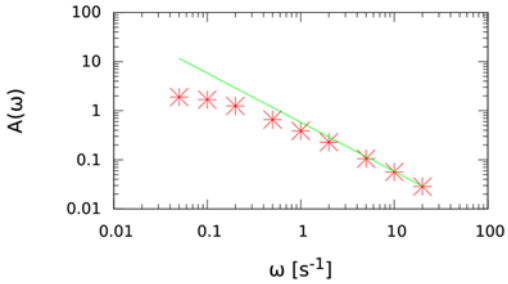

Fig. 8. Amplitude A(ω) from (16) with asymptote 0.58/ω.

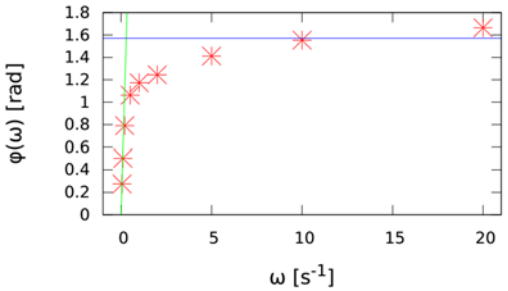

Fig. 9. Phase lag φ(ω) from (16) with line at π/2 and tangent at the origin φ = 5.5ω.

6. HEURISTICS FOR ω → ∞.

Let us first review the case of a driven solid oscillator, subject to a fluid friction force, obeying a differential equation of the form

$$\ddot{x} + \text{friction force} + \text{restoring force} = \sin\omega t \qquad (17)$$

As $\omega \to \infty$ we don't expect resonance. Therefore each term on the left-hand-side will be of order at most the order of the right-hand-side, namely $O(1)$. We expect a periodic permanent regime of period $T = 2\pi/\omega$. If the amplitude is A then $\ddot{x}$ will be of order $A\omega^2$, implying A of order at most ω^{-2}. The restoring force will be $o(1)$, the velocity of order $A\omega \sim \omega^{-1}$ and the fluid friction force $o(1)$. Therefore, as $\omega \to \infty$, the system tends to $\ddot{x} = \sin\omega t$, leading to an amplitude ω^{-2} and phase lag π, in agreement with the exact solution of the linear case.

Another driven system may obey a first order differential equation of the form

$$\dot{x} + \text{restoring force} = \sin\omega t \qquad (18)$$

Again we expect a periodic permanent regime of period $T = 2\pi/\omega$, and no resonance, so that each term on the left-hand-side will be of order at most $O(1)$. If the amplitude is A then $\dot{x}$ will be of order $A\omega$, implying A of order at most ω^{-1}. The restoring force will be $o(1)$. Therefore, as $\omega \to \infty$, the system tends to $\dot{x} = \sin\omega t$, leading to an amplitude ω^{-1} and phase lag $\pi/2$, in agreement with the exact solution of the linear case.

We have studied a drop on an oscillating incline in a regime where the inertial forces, such as the centrifugal force, are negligible with respect to gravity and capillarity, both of same order for Bond number of order one. We thus have $\omega^2 r \sim g$. The acceleration term $\partial u/\partial t$ in the Navier-Stokes equation is of same order and therefore negligible. And the Reynolds number was always less than one so that the quadratic term in the Navier-Stokes equation could be neglected. Therefore a behaviour corresponding to (18) rather than (17) should be observed, leading to an amplitude $A \sim \omega^{-1}$ rather than $A \sim \omega^{-2}$ as $\omega \to \infty$.

In simple words: a liquid drop can deform in many different ways and will do so as far as the shear stress ∇u remains bounded. If A is the amplitude of the motion of the center of mass in the frame of reference of the incline, then ∇u is of order $A\omega/r$, giving $A \sim \omega^{-1}$ as $\omega \to \infty$.

When $\omega \to 0$, acceleration is negligible in all cases, and both solid and liquid oscillators have an amplitude $O(1)$ and a phase lag $O(\omega)$.

7. CONCLUSION

A sessile millimetric droplet on an incline responds similarly to a driven damped linear oscillator to a sinusoidal oscillation of the angle of the incline. However, the amplitude of the drop deformation is proportional to ω^{-1} at large ω, whereas a simple pendulum on an oscillating incline responds with an amplitude proportional to ω^{-2} at large ω.

The diffuse interface modelisation imply diffusion times larger than the true physical times, but the discrepancy should go to zero with finer and finer meshes. Also, because there is more space for water (originally in the small sphere) to diffuse into oil (originally in the large sphere), than conversely, the level set 0.5, considered as the interface, shrinks a little during the first seconds. This effect should also go to zero with finer and finer meshes.

Beyond $\omega \sim 20 s^{-1}$, in the oscillating frame of reference, one cannot neglect the inertial pseudo-forces. One can expect that including the centrifugal force in the Navier-Stokes equation would increase the drop deformation at large ω.

REFERENCES

Boreyko, J. B. and C. H. Chen (2009). Restoring superhydrophobicity of lotus leaves with vibration-induced dewetting. *Physical Re-view Letters* 103, 174502.

Bormashenko, E., R. Pogreb, G. Whyman, and M. D. Erlich (2007). Resonance cassiewenzel wetting transition for horizontally vibrated dr ops deposited on a rough surface. *Langmuir*

23(24), 12217–12221.

Celestini, F. and R. Kofman (2006). Vibration of submillimeter-size supported droplets. *Physical Review E* 73, 041602.

Daniel, S., M. K. Chaudhury, and P. G. de Gennes (2005). Vibration-actuated drop motion on surfaces for batch microfluidic processes. *Langmuir* 21(9), 4240–4248.

De Coninck, J., F. Dunlop, and T. Huillet (2017). Contact angles of a drop pinned on an incline. *Physical Review* E 95, 052805.

Dong, L., Chaudhury, A., and Chaudhury, M. K.(2006). Lateral vibration of a water drop and its motion on a vibrating surface. *European Physical Journal E* 21(3), 231–242.

Lafaurie, B., C. Nardone, R. Scardovelli, S. Zaleski, and G. Zanetti (1994). Modelling merging and fragmentation in multiphase flows with surfer. *Journal of Computational Physics* 113, 134–147.

Le Grand, N., A. Daerr, and L. Limat (2005). Shape and motion of drops sliding down an inclined plane. *Journal of Fluid Mechanics* 541, 293–315.

Lyubimov, D. V., T. P. Lyubimova, and S. V. Shklyaev (2006). Behavior of a drop on an oscillating solid plate. *Physics of Fluids* 18(1), 012101.

Lyubimov, D., T. P. Lyubimova, and S. Shklyaev (2004, Nov). Non-axisymmetric oscillations of a hemispherical drop. *Fluid Dynamics* 39(6), 851–862.

Milne, A., B. Defez, M. Cabrerizo-Vlchez, and A. Amirfazli (2014). Understanding (sessile/constrained) bubble and drop oscillations. *Advances in Colloid and Interface Science* 203, 22 – 36.

Noblin, X., Buguin, A., and Brochard-Wyart, F. (2004). Vibrated sessile drops: Transition between pinned and mobile contact line oscillations. *European Physical Journal E* 14(4), 395–404.

Olsson, E. and G. Kreiss (2005). A conservative level set method for two phase flow. *Journal of Computational Physics* 210, 225–246.

Rahimzadeh, A. and M. Eslamian (2017). Experimental study on the evaporation of sessile droplets excited by vertical and horizontal ultrasonic vibration. *International Journal of Heat and Mass Transfer* 114, 786–795.

Vukasinovic, B., M. K. Smith, and A. Glezer (2007). Dynamics of a sessile drop in forced vibration. *Journal of Fluid Mechanics* 587, 395423.